

Enhanced photocatalytic activity of Mo- $\{001\}$ TiO₂ core-shell nanoparticles under visible light†

Xianguo Liu,^{*ab} Dianyu Geng,^{ab} Xiaolei Wang,^{ab} Song Ma,^{ab} Han Wang,^{ab} Da Li,^{ab} Baiqing Li,^{ab} Wei Liu^{ab} and Zhidong Zhang^{ab}

Received 23rd June 2010, Accepted 26th July 2010

DOI: 10.1039/c0cc02034f

Mo-TiO₂ core-shell nanoparticles are prepared by the arc-discharge method, in which anatase TiO₂ with $\{001\}$ facets are shells and Mo nanoparticles work as cores. These nanoparticles show enhanced photocatalytic activity under visible light, due to the Mo-doping in $\{001\}$ TiO₂ from diffusion at the shell-core interface.

Nanomaterials, as an intermediate state between the atomic state and bulk material, have attracted much attention due to their different and often superior properties, as compared to their bulk counterparts.^{1,2} Among the unique properties of nanomaterials, the transport properties in semiconductor nanomaterials are related to phonons which are largely affected by the size and geometry of a material.³ The high surface area brought about by a small particle size is beneficial to many TiO₂-based devices, as it facilitates reaction/interaction between the devices and the interacting media, and strongly depends on the surface area of the material.³ Usually, different facets of a single crystal with the same surface area exhibit distinct physical and chemical properties. In anatase TiO₂ crystals, they are usually dominated by $\{101\}$ facets, which are thermodynamically stable due to their low surface energy (0.44 J m⁻²). Although $\{001\}$ facets with their higher surface energy (0.90 J m⁻²) are more interesting and exhibit higher reactivity, they usually diminish rapidly during the crystal-growth process.⁴ Anatase TiO₂ with dominant $\{001\}$ facets is becoming a hot research topic, due to its promising high reactivity in heterogeneous reactions. Important progress in preparation of anatase TiO₂ single crystals with exposed $\{001\}$ facets has been achieved by Lu and co-workers, using TiF₄ as raw material.⁵ Since then, several groups have prepared these single crystals starting from other raw materials, such as fluoride, chloride, tetrabutoxide, tetraisopropoxide, *etc.* However, the raw materials mentioned above and the byproducts do pollute the environment. Very recently, anatase TiO₂ sheets with a high percentage of $\{001\}$ facets have been prepared by Lu and co-workers from titanium nitride.⁶ Unfortunately, titanium nitride is very rare and expensive, which is an obstacle for application. In this paper,

we report an easy and inexpensive route for one-step synthesis of anatase TiO₂ nanomaterials with $\{001\}$ facets.

Core-shell nanoparticles are a special type of nanoparticles, which are usually composed of a core and a shell of nanometre size that are made of different materials. Core-shell nanoparticles have been used in electromagnetic-wave-absorption devices and in ultrahigh density recording media.² As a method for producing nanoparticles, the arc-discharge technique has been widely used for the formation of core-shell nanoparticles. In previous studies, the arc-discharge technique has been used to uniformly synthesize different kinds of core-shell nanoparticles with various shell and core materials, *e.g.*, Al₂O₃-coated REAl₂ (RE = Dy, Gd, Tb, Ho) nanoparticles, carbon- and ZnO-coated nanoparticles with a core consisting of a single element, an alloy or an intermetallic compound.⁷⁻¹¹ It was also found that a high-temperature phase (like face-centered-cubic Co) can be prepared by arc discharge, which is attributed to the proper match between the energy of the high-temperature phase and that of nanoscale particles.¹² Furthermore, from the red shift of the peak at 388 nm in the fluorescence spectra of ZnO-coated Fe(Zn) solid-solution nanoparticles it has been concluded that Fe atoms diffuse at the core-shell interface.¹¹ On the basis of above results, we have used the arc-discharge technique to prepare Mo- $\{001\}$ TiO₂ core-shell nanoparticles and we have investigated the microstructure and the photocatalytic activity of these nanoparticles.

Phase analysis of the nanoparticles was performed by powder X-ray diffraction (XRD) on a D/max-2000 diffractometer with Cu-K α radiation. The detailed morphology of the nanoparticles was observed by high-resolution transmission electron microscopy (TEM JEOL-2010). UV-Visible absorption spectra were recorded using a UV-550 (Jasco, Japan). X-ray photoelectron spectroscopy (XPS) measurements were performed on an ESCALAB-250 to characterize the elemental compositions and the binding states of the Mo nanoparticles. To determine the photocatalytic activities of the nanoparticles, methylene blue (MB) was used as photodegradation target. A 13 watt fluorescent lamp was used as light source, and a filter was adopted to exclude UV light (less than 5%). The initial concentrations of the MB solutions were 20 mg l⁻¹. The dose of nanoparticles added was 3 g l⁻¹. The amount of MB in the solution was determined on the basis of its characteristic optical absorption at 665 nm using a visible light spectrophotometer (Model: 723C) based on Lambert-Beer's law.

Fig. 1(a) shows the XRD pattern of Mo-TiO₂ core-shell nanoparticles. Besides the three reflections of Mo, no reflections of oxides could be observed in the XRD pattern, indicating

^a Shenyang National Laboratory for Material Science, Institute of Metal Research, Chinese Academy of Sciences, 72 Wenhua Road, Shenyang 110016, People's Republic of China. E-mail: liuxianguo@hugh@gmail.com; Fax: (+86) 24-23891320; Tel: (+86) 24-23971859

^b International Centre for Material Physics, Chinese Academy of Sciences, 72 Wenhua Road, Shenyang 110016, People's Republic of China

† Electronic supplementary information (ESI) available: Detailed synthetic procedures. See DOI: 10.1039/c0cc02034f

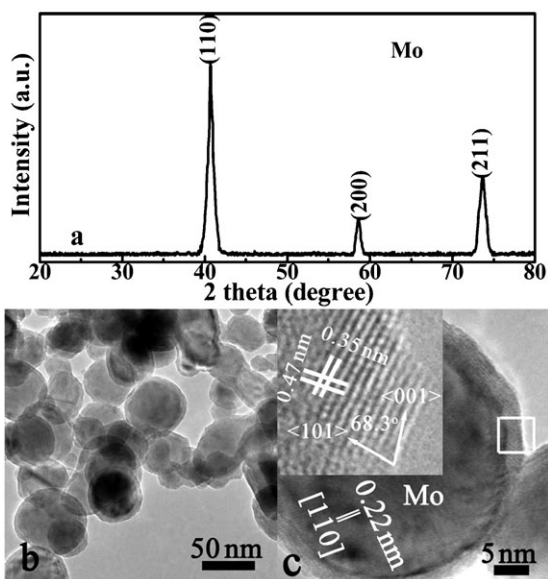


Fig. 1 (a) XRD patterns of Mo-TiO₂ core-shell nanoparticles. (b) TEM images showing the morphology of Mo-TiO₂ core-shell nanoparticles. (c) HRTEM image of a nanoparticle. The inset shows a local image of the core-shell structure within the frame of (c).

that, due to the protective shell, the Mo nanoparticles may be free from oxidation.^{7–12} The broadening of the diffraction peaks can be attributed to the relatively small sizes of the Mo nanoparticles. In the XRD pattern, there are no detectable TiO₂ reflections, indicating that its presence in the nanoparticles is less than 3%. Also the TiO₂ which forms the shell of the nanoparticles is difficult to detect in the XRD pattern because the periodic boundary condition (translation symmetry) along the radial direction has been broken down.¹⁰ Transmission electron microscopy (TEM) images of the morphologies of the nanoparticles are shown in Fig. 1(b), in which the nanoparticles are of irregular sphere-like shape and the diameter-distribution range is 30–60 nm. The average diameter and shell thickness obtained from measuring more than 300 particles are 42.6 nm and 2.4 nm, respectively. A typical HRTEM image of a Mo-TiO₂ core-shell nanoparticle, as shown in Fig. 1(c), clearly shows that it has the ‘core/shell’ type of structure with a crystalline core with a diameter of 37.6 nm and a shell with 2.2 nm thickness. In the crystalline core, the d-spacing of 0.22 nm corresponds to the lattice distance of {110} planes from XRD in Mo nanoparticles. The inset of Fig. 1(c) shows HRTEM analysis of the shell with clear crystalline lattice fringes. The fringe spacing of 0.35 nm corresponds to the {101} planes, while the fringe spacing of 0.47 nm corresponds to the {002} planes, indicating that the surface is the {001} facet. The angle between the labeled orientation indices in the inset is 68.3°, which is identical to the theoretical value for the angle between the {101} and {001} facets in an anatase.⁵ The existence of the {001} facet with high surface energy in the nanoparticles should be attributed to a proper match between the surface energy of the {001} facet and that of Mo nanoparticles.

In order to obtain more information on the surface, we investigated the nanoparticles with XPS and Raman spectra. Fig. 2(a) shows XPS patterns of binding energy (BE) with step

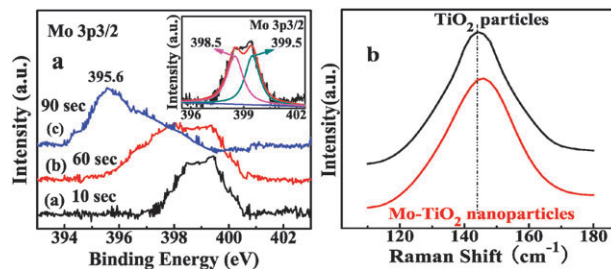


Fig. 2 (a) XPS patterns of the binding energy of Mo 3p3/2 electrons at the surface after different argon ion sputtering times of the Mo-TiO₂ core-shell nanoparticles. The inset in (a) shows the XPS spectrum and the corresponding fitting curves of Mo 3p3/2 after an etching time of 10 s. (b) Raman spectra of TiO₂ particles and Mo-TiO₂ core-shell nanoparticles.

0.5 eV for Mo 3p3/2 electrons at the surface with different argon ion sputtering times of the Mo-TiO₂ core-shell nanoparticles. The etching times of 10, 60, and 90 s, for curves (a), (b), and (c) in Fig. 2(a), correspond to the sputtering depths of about 0.3, 1.8 and 2.7 nm from the surface, respectively. The inset in Fig. 2(a) shows the XPS spectrum and the corresponding fitting curves of Mo 3p3/2 electrons at a depth of 0.3 nm, *i.e.* within the shell of the nanoparticles. The energies of 398.5 and 399.5 eV are contributed by 3p3/2 electronic state of Mo⁶⁺ state and indicate that Mo substitutes Ti in the TiO₂ as the oxide state of Mo⁶⁺ by means of diffusion at the shell-core interface. The coexistence of 398.5 and 399.5 eV is attributed to the coexistence of the amorphous and crystalline TiO₂ shell. It is observed that peaks corresponding to Mo⁶⁺ become weak with increasing etching depth and the peak at 395.6 eV, emerging after etching for 90 s to a depth of 2.7 nm and corresponding to the BE of Mo 3p3/2 in Mo, is mainly from the Mo core in the nanoparticles, further indicating that the TiO₂ shell of the nanoparticles is thinner than 2.7 nm. The Raman spectrum with large intensity at 144 cm⁻¹ arising from E_g modes in the anatase TiO₂ is presented in Fig. 2(b) and shows that there is a slight blue-shift in the Mo-TiO₂ core-shell nanoparticles compared with TiO₂ particles. Because the ionic radius of Mo⁶⁺ (0.62 Å) is somewhat smaller than that of Ti⁴⁺ (0.68 Å), lattice contraction occurs where Ti⁴⁺ is substituted by Mo⁶⁺ in the TiO₂ lattice, which results in an increase of the phonon frequency. Usually, a blue-shift of the Raman spectrum is associated with an increase of the phonon frequency.¹³ In conclusion, the blue-shift strongly indicates that the TiO₂ shell is doped by Mo. The large band gap of 3.2 eV and the high rate of electron (e⁻)-hole (h⁺) recombination prevent TiO₂ from practical application under visible light. In order to address these two problems, most of the transition metals (TM) have been doped into TiO₂ to examine their effect on the photocatalytic activity of TiO₂. TM-doping in TiO₂ nanoparticles may introduce a donor and/or acceptor level in the wide forbidden band of TiO₂, which can make the photocatalyst exhibit a response to visible light. In addition, TM elements may occur in many valence states and TM ions in the TiO₂ matrix may be potential traps of photogenerated e⁻-h⁺ pairs, lengthen the lifetime of electrons and holes and increase the photocatalytic activity. The diffusion at the interface between core and shell makes Mo enter the TiO₂ shell in

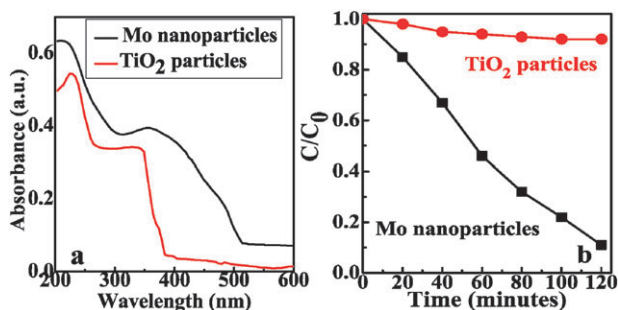


Fig. 3 (a) UV-visible absorption spectra of anatase TiO₂ particles and Mo–TiO₂ core–shell nanoparticles. (b) Variation of the MB concentration by photochemical reaction with anatase TiO₂ particles and Mo–TiO₂ core–shell nanoparticles under visible light.

the form of Mo⁶⁺, which leads to the enhanced photocatalytic activity under visible light.

Based on the XRD, TEM, XPS and Raman-spectra results above, the formation mechanism of the Mo–TiO₂ core–shell nanoparticles can be briefly summarized as follows. In the arc-discharge process, the metal atoms evaporate from the anode into the chamber, in which they react rapidly and then nucleate *via* rapid energy exchange. The boiling point and the evaporation pressure of the metals determine the amount of evaporated atoms and the sequence of condensed atoms. Ti with its boiling point of 3562 K evaporates more easily than Mo with a boiling point of 4912 K. When the temperature decreases, Mo atoms will be the first to condense. In the present experiment, Mo and Ti atoms evaporate simultaneously from the Mo₉₅Ti₅ anode, but in a certain time, more Ti atoms will enter the chamber. The evaporated Mo and Ti atoms rapidly exchange energy to form clusters in the high-temperature region of the plasma. Ti and Mo atoms form Mo (Ti) solid solution because of the similar size of these atoms. When the clusters leave the high-temperature region of the plasma, they form Mo (Ti) solid solution nanoparticles by the rapid quenching. On the other hand, similar to the formation of ZnO-coated Fe nanoparticles,¹¹ the surfaces of the Mo(Ti) solid solution nanoparticles abound with evaporated Ti atoms. After passivation, TiO₂ is formed at the surfaces of the nanoparticles giving rise to the core–shell structure.

Fig. 3(a) shows UV-visible absorption spectra of the TiO₂ particles and the Mo–TiO₂ core–shell nanoparticles. The spectrum of the TiO₂ particles exhibits the typical absorption behavior of a wide-band-gap oxide semiconductor, having an intense absorption band with a steep edge at about 390 nm. For the Mo–TiO₂ core–shell nanoparticles, a red-shift of the absorption edge is observed and the absorption tail extends to about 510 nm, which is larger than previous reports in TiO₂ nanomaterials.¹³ A red shift of light absorption in the visible region possibly leads to a better photocatalytic efficiency, especially under visible-light irradiation. It is known that the band gap of TiO₂ can be tailored by doping with some elements. The red-shift of the absorption edge due to Mo-doping in TiO₂ can be understood by the band-gap narrowing resulting from the formation of a Mo-impurity level below the conduction-band minimum of TiO₂, which is well consistent with other

reported results.¹⁵ In the present study, the photocatalytic activity of the Mo–TiO₂ core–shell nanoparticles has been evaluated in terms of the decolorization of MB dye under visible-light irradiation. The traditional commercial photocatalyst P25 is not suitable as a standard to compare with, due to distinct size difference.¹⁴ As shown in Fig. 3(b), the Mo–TiO₂ core–shell nanoparticles exhibit a much larger activity than TiO₂ particles and it is clear that the photo-reactivity is enhanced (from 8% to 89%). This is mainly due to the strong ability of the Mo–TiO₂ core–shell nanoparticles to adsorb water to form hydrogen peroxide and peroxide radicals.¹⁵ This strong ability is ascribed to the Mo-doping in TiO₂ with reactive {001} facets in the shell.

In summary, by the arc-discharge technique we have successfully prepared Mo–TiO₂ core–shell nanoparticles with TiO₂ as shell and crystalline Mo nanoparticles as core. The {001} facet has been observed for the anatase TiO₂ shell, due to the proper match between the surface energy of the TiO₂ {001} facet and that of Mo nanoparticles. Owing to the Mo doping in the TiO₂ shell with reactive {001} facets, these Mo–TiO₂ core–shell nanoparticles exhibit an absorption-edge red shift to 514 nm and enhanced photocatalytic efficiency. Therefore, they are promising as potential material for use in photovoltaic cells, photonic and optoelectronic devices, sensors and so on. At the same time, the present strategy of using the arc-discharge technique opens a new way of synthesizing other core–shell nanoparticles, in which anatase TiO₂ with exposed {001} facets act as the shells.

This work has been supported by the National Basic Research Program (No. 2010CB934603) of China, Ministry of Science and Technology of China, and the National Natural Science Foundation of China under Grant No. 50831006 and 50701045.

Notes and references

- X. B. Chen and S. S. Mao, *Chem. Rev.*, 2007, **107**, 2891.
- Z. D. Zhang, *J. Mater. Sci. Technol.*, 2007, **23**, 1.
- C. Burda, X. Chen and M. A. El-Sayed, *Chem. Rev.*, 2005, **105**, 1025.
- Y. Q. Dai, C. M. Cobley, J. Zeng and Y. N. Xia, *Nano Lett.*, 2009, **9**, 2455.
- H. G. Yang, C. H. Sun, S. Z. Qiao, J. Zou, G. Liu, S. C. Smith, H. M. Cheng and G. Q. Lu, *Nature*, 2008, **453**, 638.
- G. Liu, H. G. Yang, X. W. Wang, L. N. Cheng, J. Pan, G. Q. Lu and H. M. Cheng, *J. Am. Chem. Soc.*, 2009, **131**, 12868.
- X. G. Liu, D. Y. Geng, J. Du, S. Ma, B. Li, P. J. Shang and Z. D. Zhang, *Scr. Mater.*, 2008, **59**, 340.
- S. Ma, D. Li, W. Liu and Z. D. Zhang, *Phys. Rev. B: Condens. Matter Mater. Phys.*, 2007, **76**, 144404.
- X. G. Liu, D. Y. Geng, F. Yang and Z. D. Zhang, *J. Phys. D: Appl. Phys.*, 2009, **42**, 045008.
- X. G. Liu, D. Y. Geng, W. Liu and Z. D. Zhang, *Carbon*, 2010, **48**, 891.
- X. G. Liu, D. Y. Geng, P. J. Shang, F. Yang, B. Li and Z. D. Zhang, *J. Phys. D: Appl. Phys.*, 2008, **41**, 175006.
- S. Ma, D. Y. Geng and Z. D. Zhang, *J. Appl. Phys.*, 2005, **98**, 094304.
- K. Q. Tan, H. R. Zhang, C. F. Xie, H. W. Zheng, Y. Z. Gu and W. F. Zhang, *Catal. Commun.*, 2010, **11**, 331.
- M. Nuechter and U. Mueller, *J. Phys. Org. Chem.*, 2000, **13**, 579.
- A. Selloni, *Nat. Mater.*, 2008, **7**, 613.